Wind and Structures, Vol. 9, No. 1 (2006) 75-93
DOI: http://dx.doi.org/10.12989/was.2006.9.1.075

Interference loads of two cylinders in a side-by-side arrangement

Ewa Błazik-Borowa†

Department of Structural Mechanics, Faculty Civil and Sanitary Engineering, Lublin University of Technology, Nadbystrzycka 40, 20-618 Lublin, Poland

(Received February 1, 2005, Accepted December 28, 2005)

Abstract. This paper presents a quasi-steady model of vibrations of two cylinders in a side-by-side arrangement. The cylinders have flexible support and equal diameters. The model assumes that both cylinders participate in the process of vibration, each of them having two degrees of freedom. The movement of cylinders is described by a set of four non-linear differential equations. These equations are evaluated on the basis of a numerical simulation and experimental data. Moreover many features of cylinder vibrations are found from numerical results and are described in this paper.

Keywords: aerodynamic interference; two circular cylinders; side-by-side arrangement; quasi-steady theory; numerical experiment.

1. Introduction

Sets of two structures, which can be approximated by two circular cylinders, are often used in engineering applications e.g., chimneys, cooling towers or pipelines. Research regarding the flow around two circular cylinders has been performed since 1970 in wind tunnels (Zdravkovich and Pridden 1977, Kazakiewicz 1987, Matsumoto, Shiraishi, Shirato 1990, Ruscheweyh and Dielen 1992, Zhang and Melbourne 1995, Brika and Laneville 1995, Park and Lee 2003, Brun, Tenchine and Hopfinger 2004) and since 1990 numerically (Ng, Cheng and Ko 1997, Błazik-Borowa and Flaga 1998, Jester and Kallinderis 2003). The above research indicates that some cylinder arrangements are unstable and become subject to flow induced vibrations. A few mathematical models for such vibrations of the cylinders in tandem and staggered arrangements were proposed by Kazakiewicz (1987), Ruscheweyh and Dielen (1992), Błazik-Borowa and Flaga (1996), Bourdeix, Hémon and Santi (1998). The author of this paper has not found the mathematical models for vibrations of cylinders in a side-by-side arrangement in the literature. Hence, this paper demonstrates a mathematical model for such cylinder vibrations. It is based on the quasi-steady theory and therefore the proposed model is called quasi-steady model.

† PhD, Corresponding Author, E-mail: ebkmb@akropolis.pol.lublin.pl

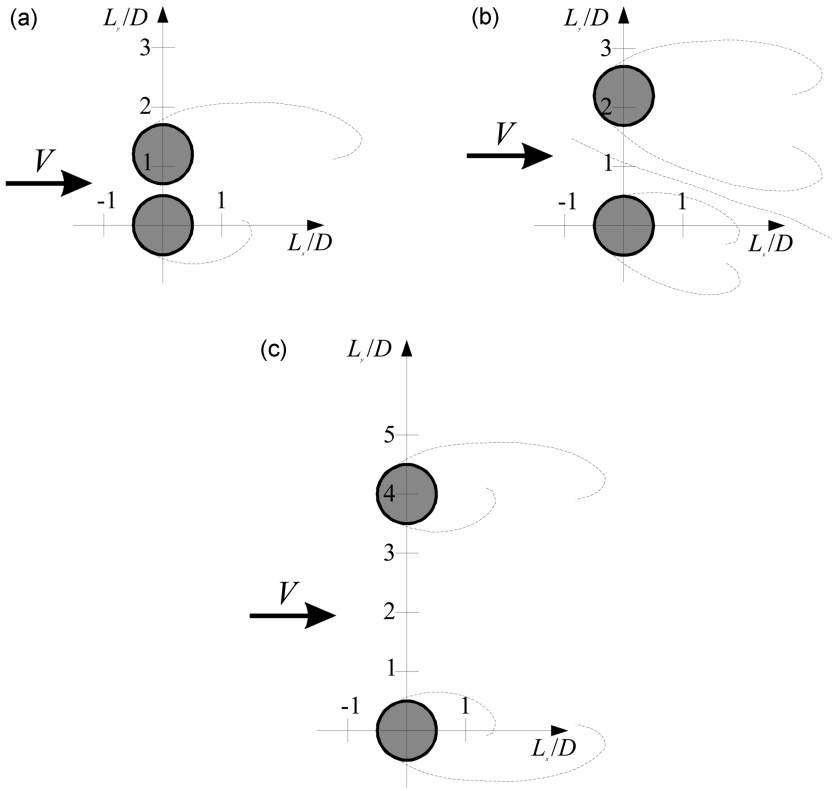

Fig. 1 Vortex paths separated from two circular cylinders in side-by-side arrangements

2. Assumptions and relations

The arrangement of two cylinders is called a side-by-side arrangement if the velocity direction is nearly perpendicular to the axis joining the midpoints of the cylinders (Fig. 1). When the distance between the centers of cylinders is $L_y = 1.2D$ the single vortex path is formed behind each as it is shown in Fig. 1(a). For the distance from $1.2D$ to $3D$, two vortex paths are created behind the cylinders. These paths are the narrow and wide wakes and they are separated by biased jet flow (Fig. 1(b)). This jet is unstable and changes sides at irregular time intervals. It causes change of pressure distributions over the cylinder surfaces and, in effect, movement of cylinders. When L_y/D is in the range from 3 to about 5 on the downstream side of cylinder two paths create and they mirror each other (Fig. 1(c)). This author theorizes that the presented mathematical model correctly describes vibrations of cylinders in the location shown in Fig. 1(b).

Most research in wind tunnel flow around cylinders is made for section models arranged respective to wind so that the problem can be treated as two-dimensional. Mathematical models, created for other phenomena of cylinder vibrations, also used the section models. Hence, one basic assumption of the proposed model of vibrations is treating cylinders as section models. Moreover, the basis of the model is the quasi-steady theory (Flaga 1994). Previously, the similar quasi-steady model was applied for analysis of interference galloping, it is vibrations of cylinders in tandem and staggered arrangements (Błazik-Borowa and Flaga 1996 and Błazik-Borowa and Flaga 1998). The

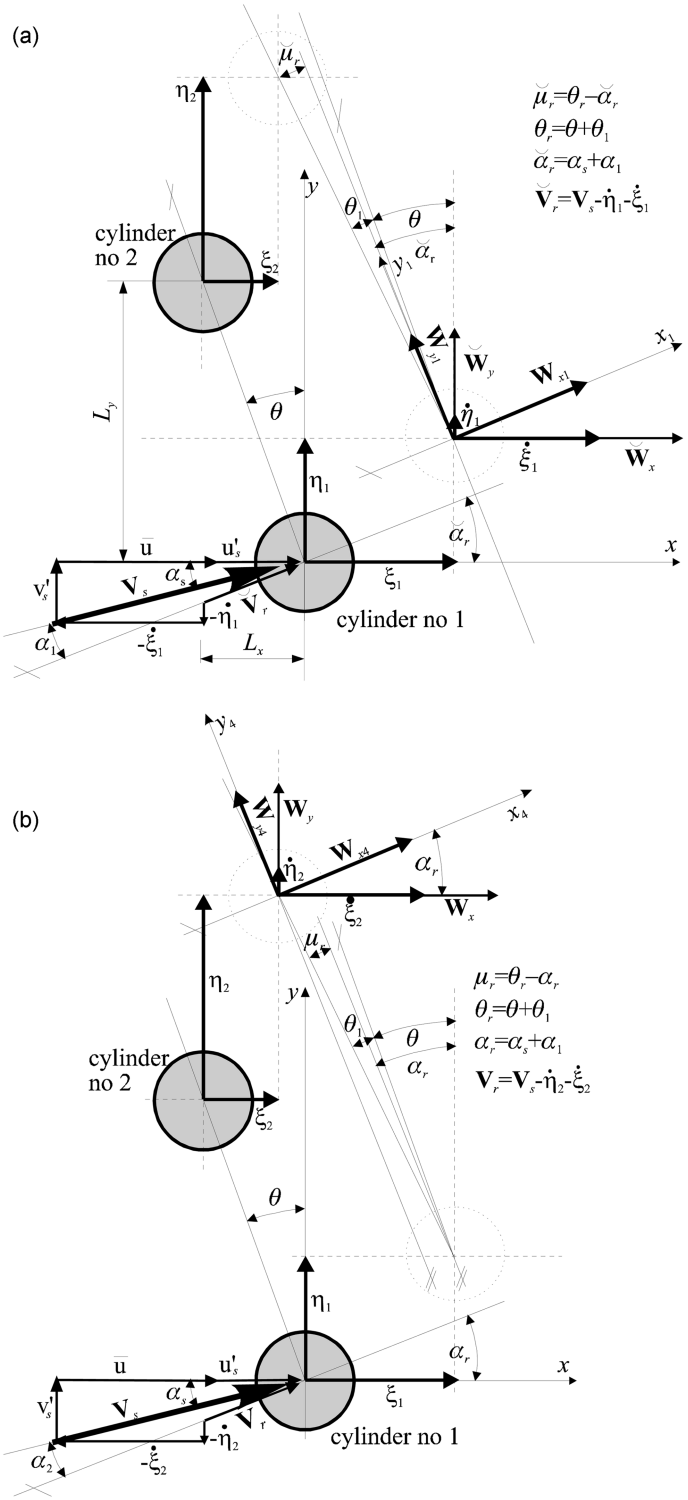

Fig. 2 The arrangements of the cylinders and basic notations

model of cylinder vibrations for the side-by-side arrangement is based on the following assumptions:

1. Diameters of crosswise intersections of cylinders are the same and equal to D.
2. Position of cylinder no. 2 is found within the region with the following limitations: $1.2 < L_y/D < 3$ and $-0.2 < L_x/D < 0.2$ (Fig. 2), that is in the region of bistable flows shown in Fig. 1(b).
3. Cylinders are made of rigid material.
4. Flow is viscous and incompressible.
5. Cylinders are elastically supported and they have two degrees of freedom: along the average wind direction and in the direction perpendicular to it.
6. Boundary disturbance effects are neglected, therefore the problem is treated as two-dimensional.
7. Global coordinate system is linked to the midpoint of cylinder no. 1 and the x axis is parallel to the average wind direction.
8. Quantities such as the instantaneous wind velocity $\mathbf{V}_s$, the components of the instantaneous wind velocity along the x and y axes: $\mathbf{u}_s$ and $\mathbf{v}_s$, the instantaneous angle of wind attack α_s, are the averaged values from the region of averaging $S = \Delta y \; x \; H$, where: H – length of cylinders; $\Delta y = \kappa_1 D$ – across dimension; $\kappa_1 \in (5 \div 10)$ (comp. Fig. 1). The spatial region of averaging is located in front of cylinders within a distance at least one D, it is in the space without disturbances caused by cylinders. This region covers the oncoming flow which influences on the forms of the wake formed behind the two cylinders.
9. Agreement with the Reynolds decomposition of the flow field components of velocity are defined by $u_s(t) = \bar{u} + u_s'(t)$ and $v_s(t) = \bar{v} + v_s'(t) = v_s'(t)$
10. Small displacements of cylinders are assumed, hence, the inertia of fluid around structures is small in comparison with the inertia of cylinders, and is ignored.
11. Other notations: $\breve{\mu}_r$, μ_r – relative angles between the directions perpendicular to the direction of relative wind velocity $\breve{\mathbf{V}}_r$ (for cylinder no. 1) and $\mathbf{V}_r$ (for cylinder no. 2), respectively, and the axis joining the midpoints of the cylinders; x_1 and y_1 – axes directed along and across the direction of the relative velocity $\breve{\mathbf{V}}_r$; x_2 and y_2 – axes directed along and across the direction of the relative velocity $\mathbf{V}_r$; ρ – fluid mass density; m – mass of one cylinder; ω_o – natural circular frequency of a cylinder; δ – damping logarithmic decrement; Sc – Scruton number defined as $Sc = \dfrac{1m\delta}{\rho D^2 H}$ Zdravkovich and Medeiros (1991); $V_r = V/\omega_o D$ – reduced velocity; $I_u = 100\%$ $\sigma/\bar{u}_w$ – turbulence intensity.

Subject to appropriate trigonometric dependence (Fig. 2), the components of wind load in respect to the global coordinate system can be given by:

- for the first cylinder

$$\breve{\mathbf{W}}_x = [\mathbf{W}_{x_1}(\breve{\mu}_r)\cos\breve{\alpha}_r - \mathbf{W}_{y_1}(\breve{\mu}_r)\sin\breve{\alpha}_r] = \cos\breve{\alpha}_r[\mathbf{W}_{x_1}(\breve{\mu}_r) - \mathbf{W}_{y_1}(\breve{\mu}_r)\tan\breve{\alpha}_r] \tag{1a}$$

$$\breve{\mathbf{W}}_y = [\mathbf{W}_{x_1}(\breve{\breve{\mu}}_r)\sin\breve{\breve{\alpha}}_r + \mathbf{W}_{y_1}(\breve{\breve{\mu}}_r)\cos\breve{\breve{\alpha}}_r] = \cos\breve{\breve{\alpha}}_r[\mathbf{W}_{x_1}(\breve{\breve{\mu}}_r)\tan\breve{\breve{\alpha}}_r + \mathbf{W}_{y_1}(\breve{\breve{\mu}}_r)] \tag{1b}$$

- for the second cylinder

$$\mathbf{W}_x = [\mathbf{W}_{x_2}(\mu_r)\cos\alpha_r - \mathbf{W}_{y_2}(\mu_r)\sin\alpha_r] = \cos\alpha_r[\mathbf{W}_{x_2}(\mu_r) - \mathbf{W}_{y_2}(\mu_r)\tan\alpha_r] \tag{2a}$$

$$\mathbf{W}_y = [\mathbf{W}_{x_2}(\mu_r)\sin\alpha_r + \mathbf{W}_{y_2}(\mu_r)\cos\alpha_r] = \cos\alpha_r[\mathbf{W}_{x_2}(\mu_r)\tan\alpha_r + \mathbf{W}_{y_2}(\mu_r)]\,; \tag{2a}$$

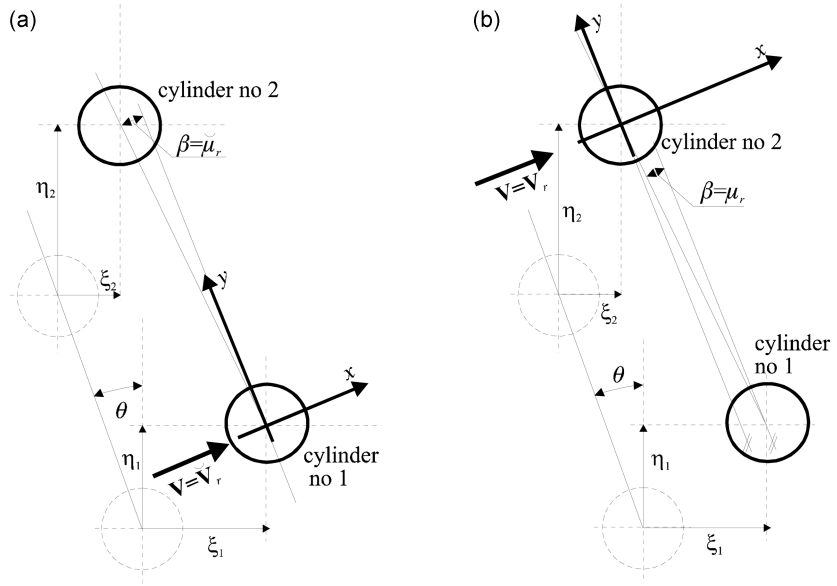

Fig. 3 The arrangement of the cylinders to evaluate static aerodynamic coefficients

where $\breve{\mathbf{W}}_{x_1}$, $\breve{\mathbf{W}}_{y_1}$ – components of load on the first cylinder along the x_1 and y_1 axes, respectively; $\mathbf{W}_{x_2}$, $\mathbf{W}_{y_2}$ – components of load on the second cylinder along the x_2 and y_2 axes, respectively.

On the basis of dimensional analysis and the quasi-steady theory, the above components of aerodynamic load can be described as functions of static aerodynamic drag and lift coefficients:

$$W_i(\bar{\mu}_r) = \frac{1}{2}\rho \bar{V}_r^2 D C_i(\bar{\mu}_r);\ C_i(\bar{\mu}_r) = \breve{C}_j(\beta = \bar{\mu}_r);\ i = x_1, y_1; j = x, y \tag{3}$$

$$W_i(\mu_r) = \frac{1}{2}\rho V_r^2 D C_i(\mu_r);\ C_i(\mu_r) = C_j(\beta = \mu_r);\ i = x_2, y_2; j = x, y \tag{4}$$

The $\breve{C}_x(\beta)$, $\breve{C}_y(\beta)$, $C_x(\beta)$ and $C_y(\beta)$ coefficients are obtained for the set of fixed cylinders and the constant wind velocity (so called steady flow) as shown in Fig. 3. The arrangement of these cylinders corresponds to the momentary arrangement of vibrating cylinders. The aerodynamic coefficients have been adopted from Zdravkovich and Pridden (1977) and ESDU 84015 (1984). They are defined in terms of the angle β and represented by a polyline for angles from –40 to 40 degrees. Exemplary graphs of aerodynamic coefficients for the subcritical range of Reynolds number are shown in Fig. 4÷7. The graphs of drag coefficients for the first and second cylinders are symmetric with respect to the axis of ordinates. The graphs of lift coefficients are central symmetric respective to points which are common for the axis of ordinates and the graphs. Most graphs describing aerodynamic coefficients have rapid jumps around $\beta = 0^o$. These sudden changes of aerodynamic forces are responsible for unstable moving cylinders.

The relative angles of the wind attack are described by an equations:

- for the first cylinder (see Fig. 2(a))

$$\bar{\mu}_r(t) = ((\theta + \theta_1(t)) - (\alpha_s(t) + \alpha_1(t))) = \theta_r(t) - \bar{\alpha}_r(t) \tag{5a}$$

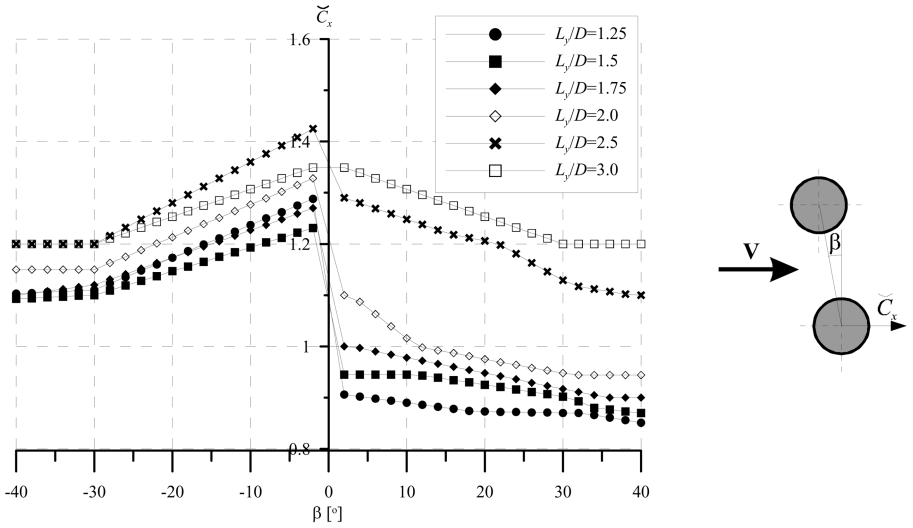

Fig. 4 The graphs of the drag coefficient for the cylinder no 1 at $Re=6\cdot10^4$ adopted from Zdravkovich and Pridden (1977) and ESDU 84015 (1984)

$$\bar{\alpha}_r(t) = \arctan\frac{v_s'(t)-\dot{\eta}_1(t)}{u_s(t)-\dot{\xi}_1(t)} \tag{5b}$$

$$\bar{\mu}_r(t) = \arctan\frac{(L_y\tan\theta-\xi(t))(u_s(t)-\dot{\xi}_1(t))-(v_s'(t)-\dot{\eta}_1(t))(L_y+\eta(t))}{(u_s(t)-\dot{\xi}_1(t))(L_y+\eta(t))+(L_y\tan\theta-\xi(t))(v_s'(t)-\dot{\eta}_1(t))} \tag{5c}$$

- for the second cylinder (see Fig. 2b)

$$\mu_r(t) = (\theta+\theta_1(t))-(\alpha_s(t)+\alpha_2(t)) = \theta_r(t)-\alpha_r(t) \tag{6a}$$

$$\alpha_r(t) = \arctan\frac{v_s'(t)-\dot{\eta}_2(t)}{u_s(t)-\dot{\xi}_2(t)} \tag{6b}$$

$$\mu_r(t) = \arctan\frac{(L_y\tan\theta-\xi(t))(u_s(t)-\dot{\xi}_2(t))-(v_s'(t)-\dot{\eta}_2(t))(L_y+\eta(t))}{(u_s(t)-\dot{\xi}_2(t))(L_y+\eta(t))+(L_y\tan\theta-\xi(t))(v_s'(t)-\dot{\eta}_2(t))} \tag{6c}$$

- for both cylinders

$$\theta_r(t) = \arctan\frac{L_y\tan(\theta)-\xi(t)}{L_y+\eta(t)} \tag{7}$$

where θ – angle between the directions perpendicular to the direction of the averaged wind velocity $\bar{\mathbf{u}}$ and the axis joining the midpoints of the fixed cylinders; θ_1 – increase of the θ angle coming from changes of cylinder locations; θ_r – angle between the directions perpendicular to the direction of the averaged wind velocity $\bar{\mathbf{u}}$ and the axis joining the midpoints of the moved cylinders; α_1, α_2 – increases of the α_s angle coming from velocity vectors of cylinders; $\bar{\alpha}_r(t)$, $\alpha_r(t)$ – angles between the direction of the averaged wind velocity $\bar{\mathbf{u}}$ and the directions of relative wind velocities,

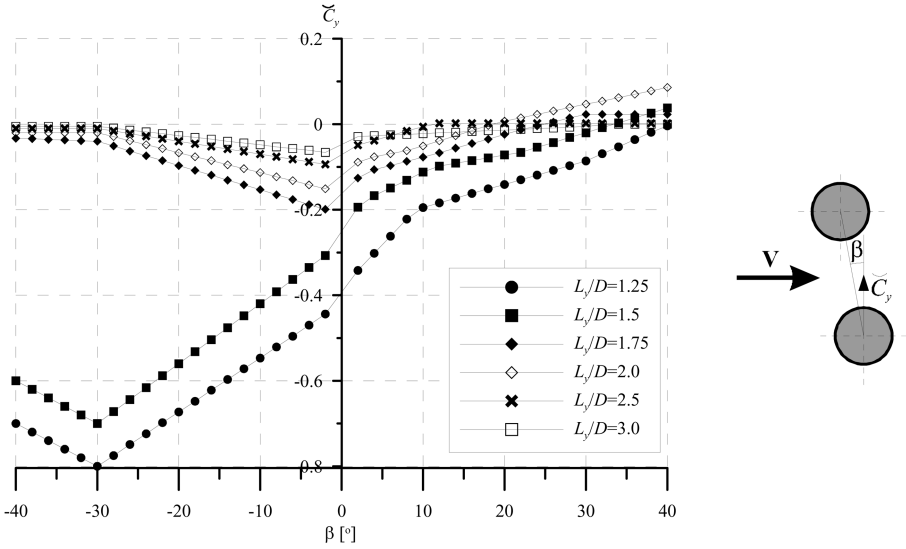

Fig. 5 The graphs of the lift coefficient for the cylinder no 1 at $Re = 6 \cdot 10^4$ adopted from Zdravkovich and Pridden (1977) and ESDU 84015 (1984)

respectively, $\bar{\mathbf{V}}_r$ and $\mathbf{V}_r$; ξ_1, η_1, ξ_2, η_2 – components of displacements for the first and second cylinders towards the x and y axes, respectively; $\xi = \xi_2 - \xi_1$; $\eta = \eta_2 - \eta_1$.

Final Eqs. (5c) and (6c) are derived by subtracting the arctangent functions of corresponding angles. Eq. (5b) should be subtracted from Eq. (7) in order to obtain Eq. (5c), and Eq. (6b) from Eq. (7) to obtain Eq. (6c).

The vectors of the relative velocities are defined as (Fig. 2):

$$\bar{\mathbf{V}}_r(t) = \mathbf{V}_s(t) - \dot{\boldsymbol{\eta}}_1(t) - \dot{\xi}_1(t) \text{ for the first cylinder} \tag{8}$$

$$\mathbf{V}_r(t) = \mathbf{V}_s(t) - \dot{\boldsymbol{\eta}}_2(t) - \dot{\xi}_2(t) \text{ for the second cylinder} \tag{9}$$

It can be noted that

$$\bar{V}_r^2(t)\cos\bar{\alpha}_r = (u_s(t) - \dot{\xi}_1(t))\sqrt{(u_s(t) - \dot{\xi}_1(t))^2 + (v_s'(t) - \dot{\eta}_1(t))^2} \text{ and} \tag{10}$$

$$V_r^2(t)\cos\alpha_r = (u_s(t) - \dot{\xi}_2(t))\sqrt{(u_s(t) - \dot{\xi}_2(t))^2 + (v_s'(t) - \dot{\eta}_2(t))^2} \tag{11}$$

Taking into consideration Eq. (1)÷(4), Eq. (10) and Eq. (11) we obtain the following formulae for the wind loads:

- for the first cylinder

$$\bar{W}_x(t) = 0.5\rho D \times$$

$$[C_{x_1}(\bar{\mu}(t))(u_s(t) - \dot{\xi}_1(t)) - C_{y_1}(\bar{\mu}(t))(v_s'(t) - \dot{\eta}_1(t))]\sqrt{(u_s(t) - \dot{\xi}_1(t))^2 + (v_s'(t) - \dot{\eta}_1(t))^2} \tag{12}$$

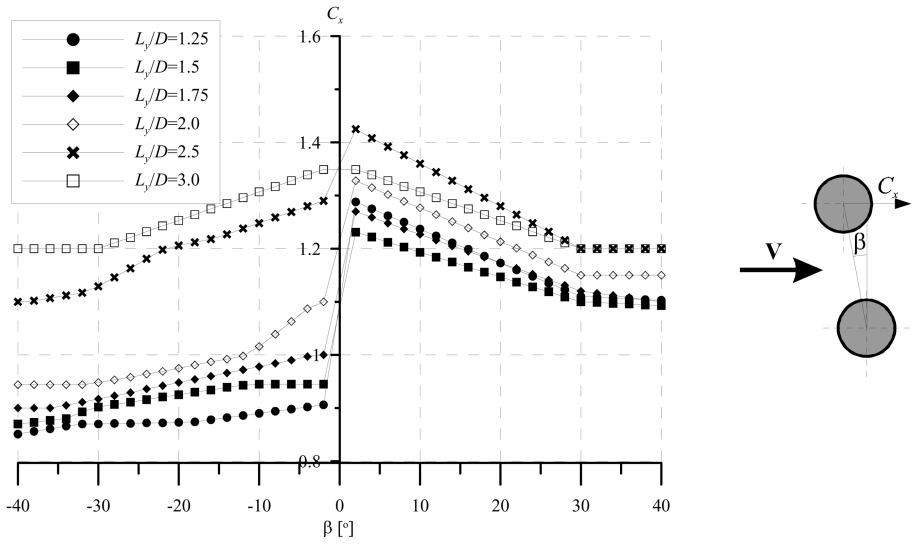

Fig. 6 The graphs of the drag coefficient for the cylinder no 2 at $Re = 6 \cdot 10^4$ adopted from Zdravkovich and Pridden (1977) and ESDU 84015 (1984)

$$\bar{W}_y(t) = 0.5\rho D \times$$

$$[C_{x_1}(\bar{\mu}(t))(v_s'(t) - \dot{\eta}_1(t)) + C_{y_1}(\bar{\mu}(t))(u_s(t) - \dot{\xi}_1(t))]\sqrt{(u_s(t) - \dot{\xi}_1(t))^2 + (v_s'(t) - \dot{\eta}_1(t))^2} \quad (13)$$

- for the second cylinder

$$W_x(t) = 0.5\rho D \times$$

$$[C_{x_2}(\mu(t))(u_s(t) - \dot{\xi}_2(t)) - C_{y_2}(\mu(t))(v_s'(t) - \dot{\eta}_2(t))]\sqrt{(u_s(t) - \dot{\xi}_2(t))^2 + (v_s'(t) - \dot{\eta}_2(t))^2} \quad (14)$$

$$W_y(t) = 0.5\rho D \times$$

$$[C_{x_2}(\mu(t))(v_s'(t) - \dot{\eta}_2(t)) + C_{y_2}(\mu(t))(u_s(t) - \dot{\xi}_2(t))]\sqrt{(u_s(t) - \dot{\xi}_2(t))^2 + (v_s'(t) - \dot{\eta}_2(t))^2} \quad (15)$$

3. Equations of motion

The equations describing the movement of these cylinders along x-axis (the average wind direction) and y-axis (direction perpendicular to average wind direction) are formulated according to an assumption that each cylinder has two degrees of freedom. The right sides of these equations are the sums of acceleration, damping, and stiffness forces. The left sides are equal to wind loads. The motion equations can be written in the set of four non-linear differential equations:

- for the first cylinder

$$m\ddot{\xi}_1(t) + C_{\xi_1}\dot{\xi}_1(t) + K_{\xi_1}\xi_1(t) = \bar{W}_x(t); \quad m\ddot{\eta}_1(t) + C_{\eta_1}\dot{\eta}_1(t) + K_{\eta_1}\eta_1(t) = \bar{W}_y(t) \quad (16)$$

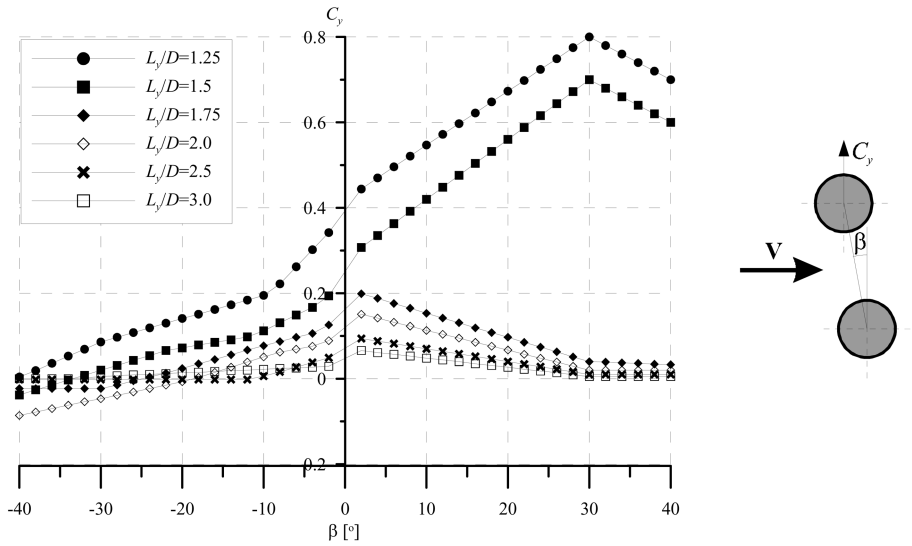

Fig. 7 The graphs of the lift coefficient for the cylinder no 2 at $Re = 6 \cdot 10^4$ adopted from Zdravkovich and Pridden (1977) and ESDU 84015 (1984)

- for the second cylinder

$$m\ddot{\xi}_2(t) + C_{\xi_2}\dot{\xi}_2(t) + K_{\xi_2}\xi_2(t) = W_x(t); \quad m\ddot{\eta}_2(t) + C_{\eta_2}\dot{\eta}_2(t) + K_{\eta_2}\eta_2(t) = W_y(t) \tag{17}$$

where: K_{ξ_1}, K_{η_1}, K_{ξ_2}, K_{η_2}, C_{ξ_1}, C_{η_1}, C_{ξ_2}, C_{η_2} –damping and stiffness coefficients for the first and second cylinder towards the x and y axes, respectively; $\tilde{W}_x(t)$, $\tilde{W}_y(t)$ $W_x(t)$, and $W_y(t)$ – components of wind loads described by Eq. (12)÷(15).

4. The numerical analyses of cylinder vibrations

4.1. Calculation method

The system of four differential equations of the second order, as discussed above, can be replaced by a system of eight equations of the first order and solved numerically with Runge-Kutta's method. Damping coefficients are described by equations:

$$C_{\xi_1} = C_{\eta_1} = C_{\xi_2} = C_{\eta_2} = 2\delta m\omega_o, \tag{18}$$

and are conditions by the Scruton number.

In order to check the quasi-steady model for the side-by-side arrangement numerical analyses are undertaken for the three cases:

- first group of data similar to ropes of the cable-stayed bridge in Praha (from Studnićková 1994) – $D = 0.168$ m, $m = 87.7$ kg, $\omega_o = 6.41$ rad/s, $K_{\xi_1} = K_{\eta_1} = K_{\xi_2} = K_{\eta_2} = 3000$ N/m, $I_u = 0$, $I_u = 1\%$, $I_u = 12.8\%$, δ depends on the Scruton number, $Sc \in (10,100)$ $\rho = 1.25$ kg/m^3;
- second group of data adopted from Gowda, Sreedharan and Narayanan (1993) – $D = 0.012$ m, $m = 0.0116$ kg, $\omega_o = 345.6$ rad/s, $I_u = 1\%$, $K_{\xi_1} = K_{\eta_1} = 4.1 \cdot 10^6$ N/m, $K_{\xi_2} = 400$ N/m, $K_{\eta_2} = \omega_o^2 m = 1385$

N/m, $\delta = 0.003$, $Sc = 3$, $\rho = 1.25$ kg/m^3;

- third group of data adopted from Ikegami, Fujita and Ohashi (1993) – $D = 0.01$ m, $m = 0.0617$ kg, $\omega_o = 3000$ rad/s, $I_u = 0\%$, $K_{\xi_1} = K_{\eta_1} = K_{\xi_2} = K_{\eta_2} = 1.7 \cdot 10^5$ N/m, $\delta = 0.55$, $Sc = 6.7$, $\rho = 1000$ kg/m^3 (as for water).

In most data given in papers, the authors do not give the stiffness K_i. For the first group, the stiffness of cylinders is evaluated as forces induce unit displacement of ropes. In the research of Gowda, Sreedharan and Narayanan (1993), the first cylinder is fixed at the ends, and the second cylinder is supported by vertical springs. For the first cylinder the stiffness K_{ξ_1} and K_{η_2} are calculated as forces induce unit displacement in middle of bars. The stiffness K_{η_2} is evaluated for a body with one degree of freedom, and the horizontal stiffness K_{ξ_2} is assumed as part of the vertical stiffness. For the last group of data, the natural frequencies and stiffness are calculated for the bar fixed at one end.

The u_s and v_s' components of the wind velocity are averaged values from ten correlated random processes, which are generated in ten points forming a plane in front of cylinders. The WAWS (Weighted Amplitude Wave Superposition) and ARMA (Auto-Regresive Moving Average) methods were used to generate these random processes. These methods are described in many papers, for example, Shinozuka and Jan (1972), Borri, Crocchini, Facchini and Spinelli (1995), Błazik-Borowa and Szulej (2004).

The results shown in Fig. 8 and Fig. 11 ÷ 16 are obtained for the first group of data. Fig. 9 is prepared for the second group of data and Fig. 10 for third group.

4.2. The numerical verification

The numerical analyses are preceded by the numerical verification of the mathematical phenomenon model. Fig. 8 shows a comparison of numerical and experimental results obtained under flow conditions with a turbulence intensity $I_u = 1\%$. The experimental data is from Zdravkovich and Medeiros (1991). In Fig. 8 the rapid increase of vibration amplitudes at some reduced velocity V_r is shown. This reduced velocity is called the critical reduced velocity V_{cr} by Zdravkovich and Medeiros (1991), similarly as for the galloping phenomenon. As it is demonstrated, the reduced critical velocities obtained from calculations are smaller than measured in the wind tunnel, whereas, the values of calculated amplitudes are insignificantly bigger than measured ones. Analysed parameters both from calculations and research in the wind tunnel are of the same order. Differences come from disturbances around ends of cylinders existing in the wind tunnel. In the tunnel the analysed wind load does not act on whole cylinders, but only on their parts. Their lengths depend on a wind tunnel and they can be equal to about 70% of the whole cylinder's length as it is described by Gowda, Sreedharan and Narayanan (1993). Additionally, disturbances at the ends damp vibrations. In effect, in the wind tunnel greater wind velocity induces vibrations, and cylinders have smaller amplitudes than it is expected from theory.

All research shows that the cylinder vibrations exist for the limited range of velocities. It seems to be an attribute of phenomena. It is not obtained in numerical research shown in Fig.8, because further calculations need significantly bigger velocities. But it is obtained in the next calculations for the second group of data (Fig. 9). In Fig. 9, the difference between reduced velocities, for which the vibrations vanish, is shown. As for earlier comparison, these differences come from distributions around ends of cylinders existing in the wind tunnel. Additionally, the stiffness K_{ξ_2} is not given in the paper of Gowda, Sreedharan and Narayanan (1993) and the assumed stiffness in the calculation can distinguish from the value from the research in the wind tunnel.

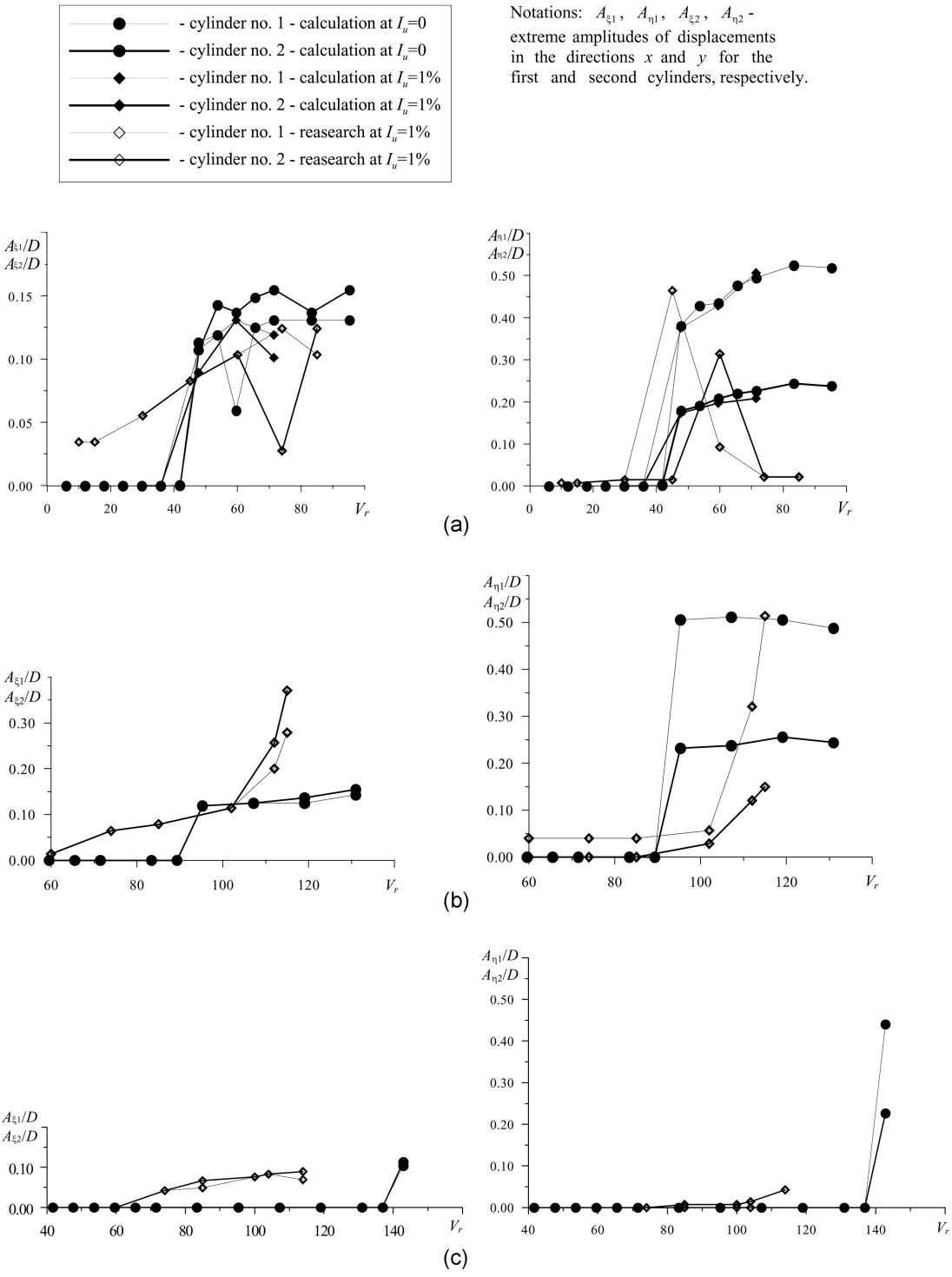

Fig. 8 The comparison of numerical results and research from the paper of Zdravkovich and Medeiros (1991) at $L_y/D=1.2$ and $\theta=5^o$ for the first group of data; (a) $Sc=10$; (b) $Sc=50$; (c) $Sc=100$

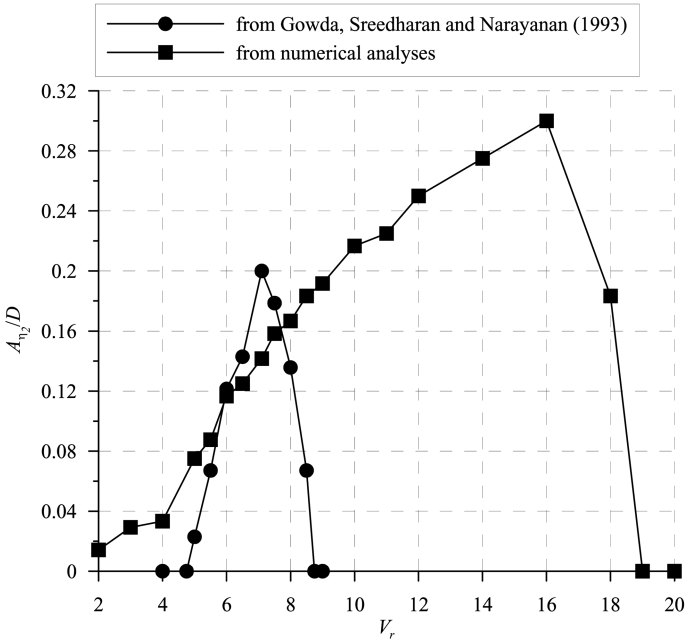

Fig. 9 The comparison of numerical results and research from the paper of Gowda, Sreedharan and Narayanan (1993) at $L_y/D=1.3$ and $\theta=0^o$ for the second group of data

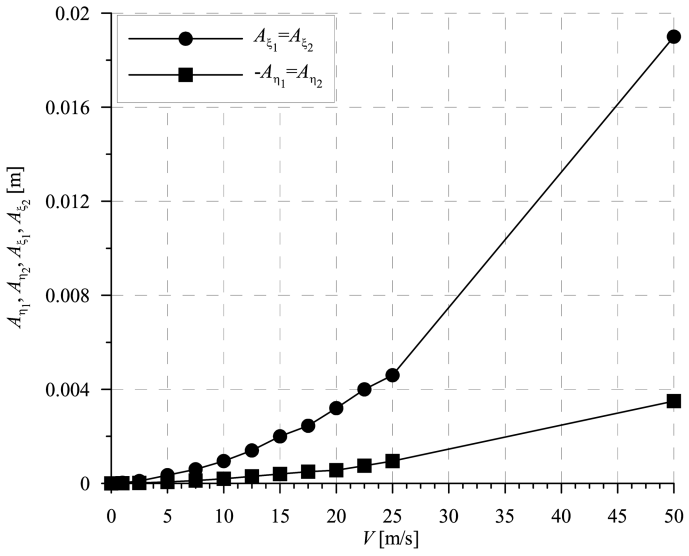

Fig. 10 The graphs of amplitudes of vibrations as functions of the water velocities at $L_y/D=1.6$ and $\theta=0^o$ for the third group of data

Ikegami, Fujita and Ohashi (1993) measured acceleration of vibrating cylinders in three types of arrangements. The vibrations were induced by the water jet. Authors created relations of acceleration amplitudes and water velocities and, on this basis, they determined the critical

velocities at which vibrations start. For the side-by-side arrangement, the critical velocity is equal to 6 m/s. For water velocity bigger than 10 m/s, the values of accelerations are in the range from 20 g to 40 g (where g is the acceleration of gravity). Fig. 10 shows the numerical results. The graphs of vibration amplitudes do not show rapid change which may be responsible for existing critical

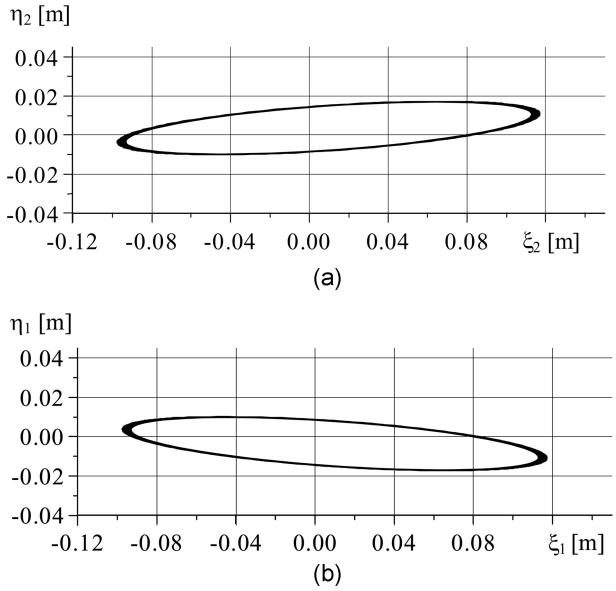

Fig. 11 Trajectory forms of cylinders at the steady flow with $V_s = \bar{u} = 16$ m/s and $L_y/D = 1.2$, $\theta = 0^o$, $Sc = 50$ for the first group of data

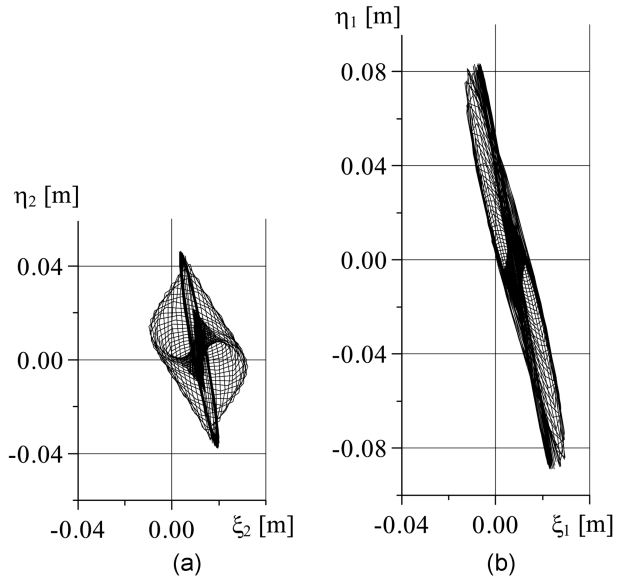

Fig. 12 Trajectory forms of cylinders at the steady flow with $V_s = \bar{u} = 16$ m/s and $L_y/D = 1.2$, $\theta = 5^o$, $Sc = 50$ for the first group of data

velocity of vibrations. For the velocity $V=15$ m/s the accelerations are calculated. For the vibrations towards the axis x, it is equal to 23 g and for the vibrations towards the axis $y-3.5$ g. Differences between the calculations and research probably come both from disturbances at the ends and from the big inertia of water. One of the assumptions of the presented model is neglecting the inertia of flow. It means that the model cannot be applied for the flow of water around cylinders, but earlier comparisons show that it can be applied for wind loads where air flows around cylinders.

4.3. The numerical research

From above comparison it can be found that the proposed mathematical model properly describes vibrations of cylinders in side-by-side arrangement caused by the flow of air. Hence, further calculations have been done and their results are used to analyse the described phenomenon.

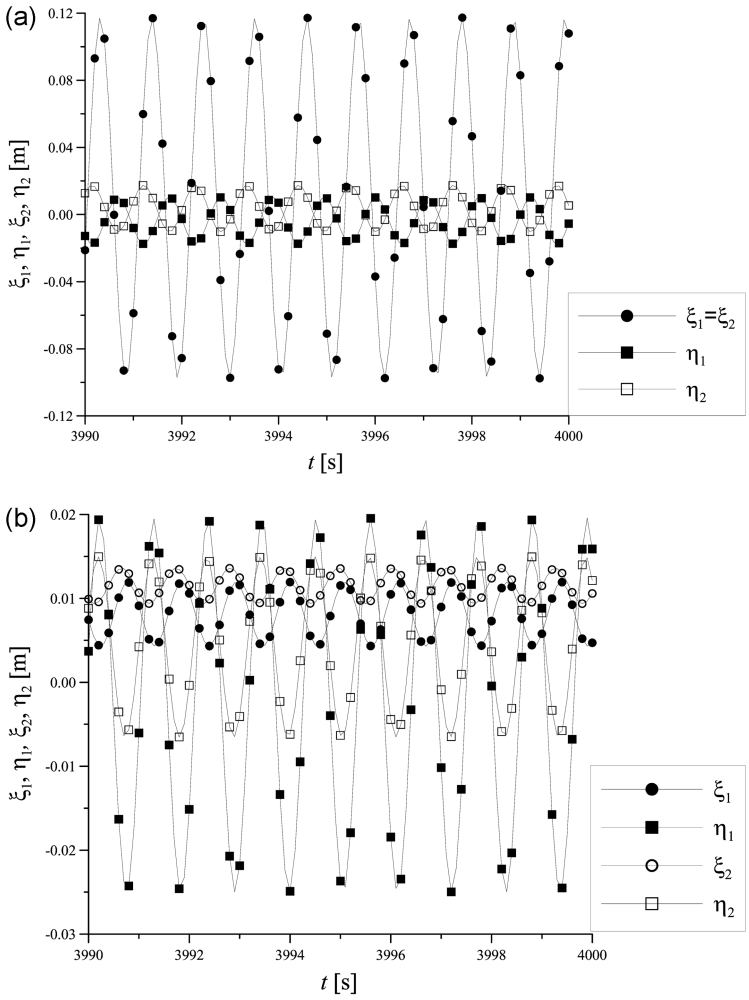

Fig. 13 The vibrations of cylinders at steady flow and $V_s=\bar{u}=16$ m/s, $Sc=50$, $L_y/D=1.2$ for the first group of data; (a) $\theta=0^o$; (b) $\theta=5^o$

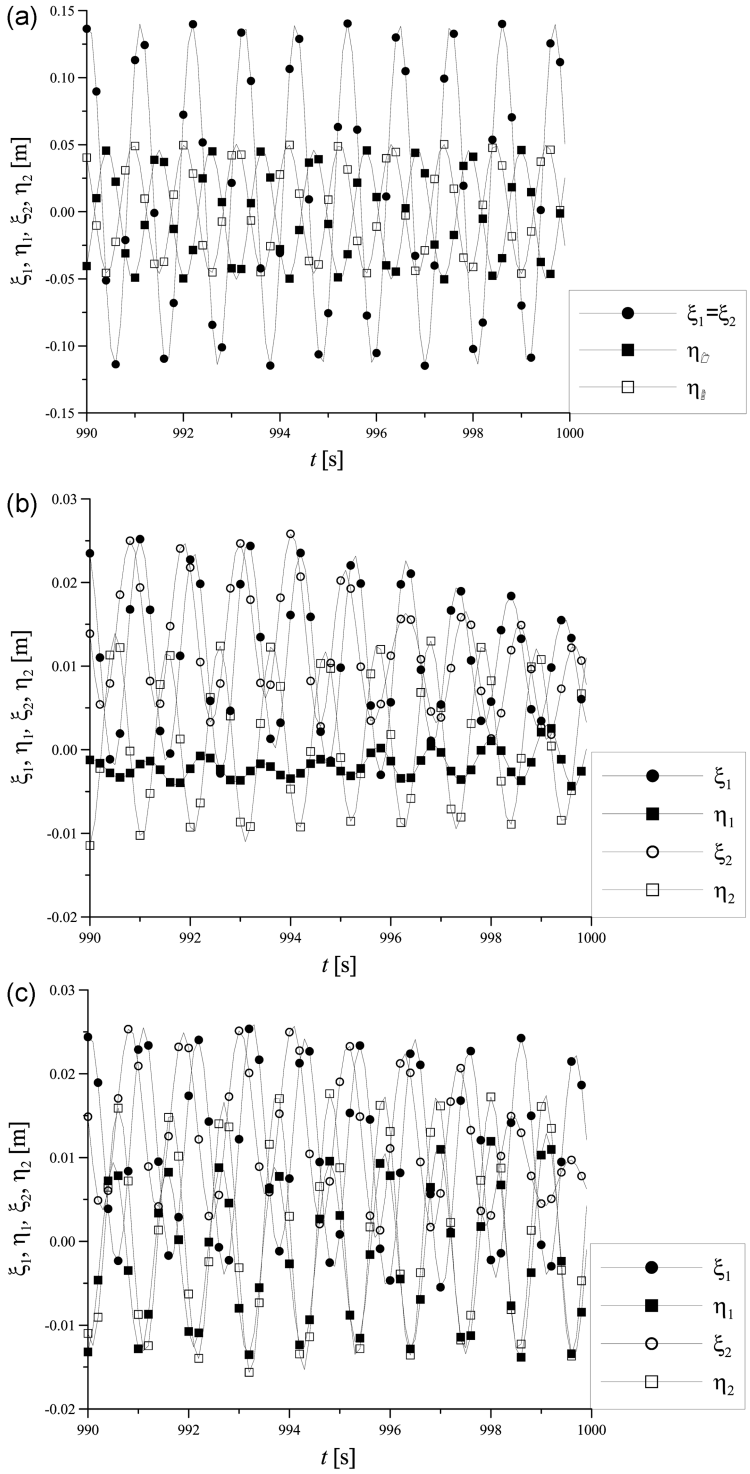

Fig. 14 The vibrations of cylinders at steady and unsteady flows with $\bar{u}=18$ m/s, $Sc=50$, $L_y/D=1.75$ for the first group of data; (a) $\theta=0^o$, $I_u=0\%$; (b) $\theta=0^o$, $I_u=12.8\%$; (c) $\theta=5^o$, $I_u=12.8\%$

Fig. 11 shows trajectories for cylinders located perpendicular to the wind direction, that is $\theta=0^{o}$, and at steady flow. Both cylinders move along similar and regular ellipses. In the case of the cylinders situated in other way (e.g., $\theta=5^{o}$), trajectories of cylinders become less regular and amplitudes of vibration differ considerably (Fig. 12). Differences between vibrations of cylinders arranged so that $\theta=0^{o}$ and $\theta=5^{o}$ are shown also in Fig. 13. Here it is seen for $\theta=0^{o}$ that vibrations towards the x axis have the same values and phases, components of vibrations towards the y axis also have the same phases and values of displacement, but the displacement vectors have the opposite sense (comp. also Fig. 14a). The amplitudes of vibrations along the x axis are bigger than across one. Whereas for $\theta=5^{o}$ the amplitudes of vibrations along the x axis are smaller than across one and both components of vibrations towards the x and y axes have no common phases.

It can be noted that the solution of the set of differential Eq. (16) and (17) for the steady flow is periodic. We can distinguish two types of periods: the period between extreme amplitudes and the period of vibration, as shown in Fig. 15 for significantly longer time than in previous figures. The cylinders move back to their previous trajectory after a time delay, which is equal to the period.

Fig. 16 represents the relationship between the Scruton numbers Sc, critical reduced velocities V_{cr} and cylinder locations at steady flow. It is seen that the critical reduced velocity nearly linear depends on the Scruton number. For the arrangement of cylinders with $\theta=0^{o}$ the graph is

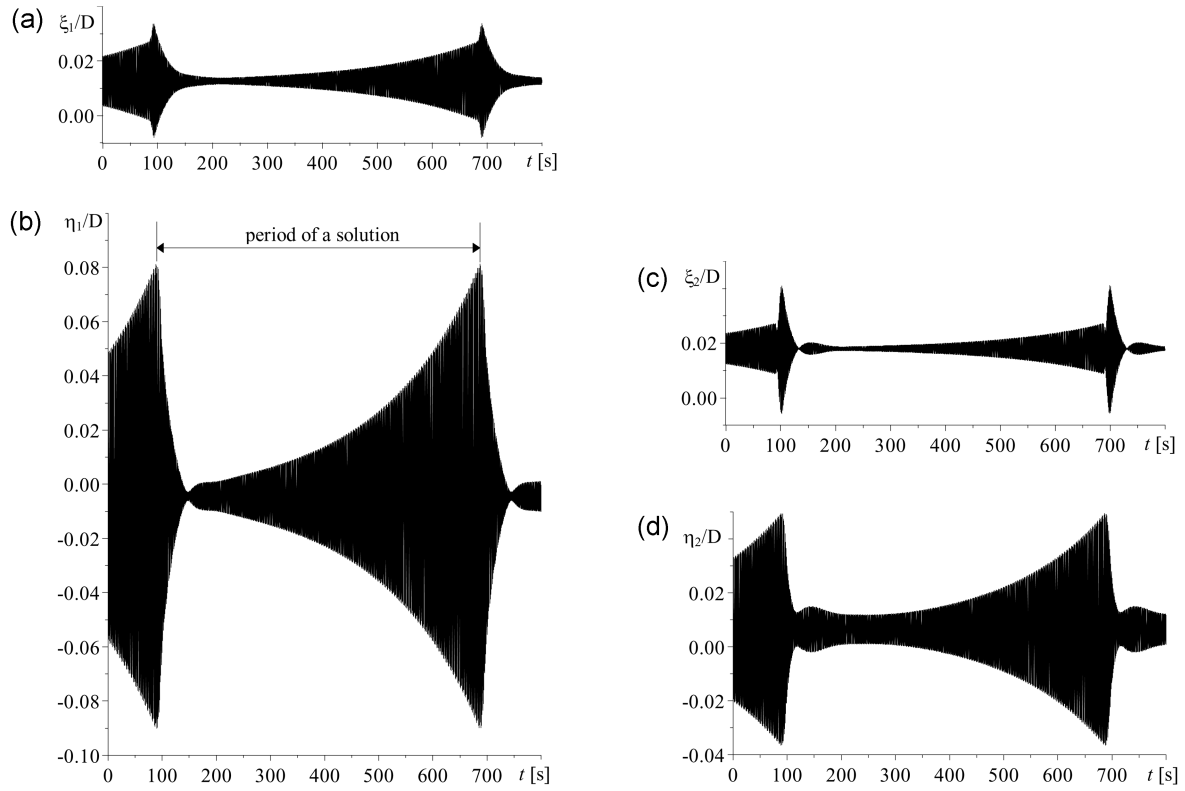

Fig. 15 Relative displacements of cylinders as functions of time at the steady flow $V_s=\bar{u}=20$ m/s and $L_y/D=1.2$, $\theta=5^{o}$, $Sc=50$ for the first group of data

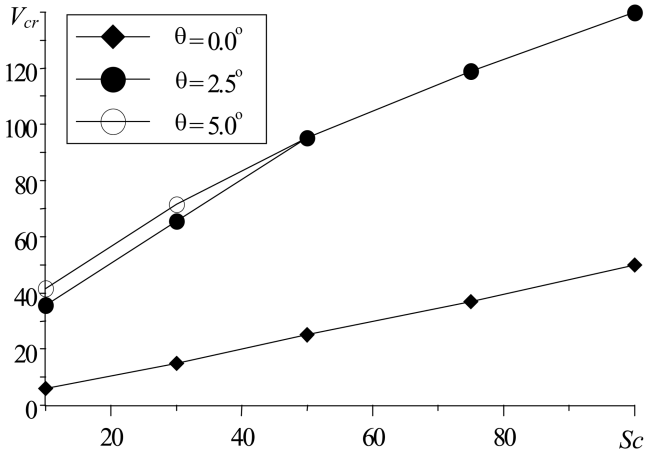

Fig. 16 The critical reduced velocity of cylinder vibration as function of the Scruton number and the cylinder location at the steady flow and $L_y/D=1.2$ for the first group of data

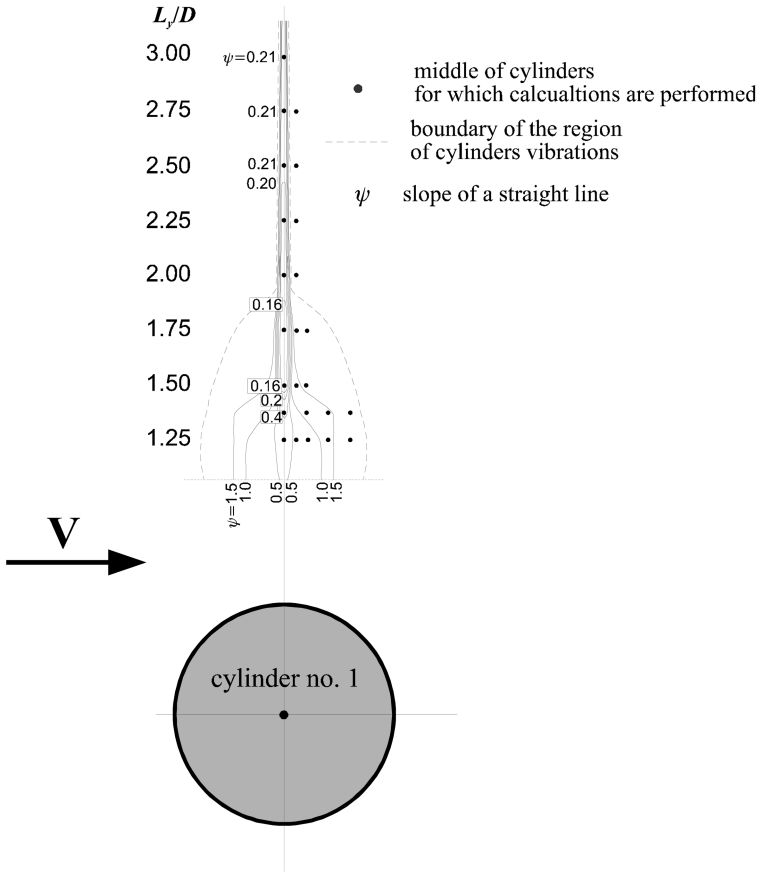

Fig. 17 The region of arrangements of cylinders for which can exist vibrations

significantly below others and the slope angle of this graph is small. It means the vibrations of cylinders arranged along the y axis are rather easily induced. It is also shown in previous figures.

Finally, the region of cylinder arrangements for which vibrations at steady flow can be induced is shown in Fig. 17. There are lines joining points of the same value of the ψ coefficient which is the slope of a straight line described by the following equation

$$Vcr = \psi Sc + A \tag{19}$$

Above formulae is obtained from the interpolation of the relationship between the Scruton number Sc and the critical reduced velocity V_{cr} with use of the minimum mean-square method. It should be noted that cylinder vibrations are more possible at the smaller values of the ψ coefficient. In Fig. 17 the drop line is the boundary of the region of existing vibrations for the steady flow.

Research of possibilities of existing vibrations show that at steady flow in the checked region, it is for $1.2 < L_y/D < 3$, cylinders vibrate for $\theta = 0^o$ (Fig. 11, Fig. 14a, Fig. 17). For $L_y/D > 2.0$ and $\theta \neq 0^o$ vibrations cannot be induced at steady flow. Excitation of vibrations in this location is possible at unsteady flow. In this situation amplitudes of vibrations are significantly smaller, but they exist for all side-by-side arrangements in the region limited by $1.2 < L_y/D < 3$ and $-0.4 < L_x/D < 0.4$, it is in the region bigger than it is assumed in p. 2.

5. Conclusions

The comparison of numerical analyses and wind tunnel research presented in Fig. 8 and Fig. 9 shows similar cylinder vibrations induced by wind velocity. It can, therefore, be concluded that the quasi-steady model can serve as a reasonable tool to describe the vibrations of two cylindrical structures in side-by-side arrangement in civil engineering. Thus, this model could be useful in determining the safe distance between cylinders. Also note, the critical velocity of wind induced vibrations depends on the Scruton number, as well as the turbulence intensity of wind flow. For analysed arrangements the region of unstable locations of cylinders at steady flow is shown in Fig. 17.

The last stage of modelling an aerodynamic interference for cylinders in side-by-side arrangement takes into consideration boundary distributions. The proposed model properly describes vibrations of slender and long ropes (for example, ropes of cable-stayed bridges), but for chimneys, cooling towers, etc. the model gives lesser values for critical velocities and greater amplitudes. It comes from that the wind distribution load acts on the whole cylinder's length in the theoretical model, but for real structures this load has the same value but it acts only on the part of building. Of course, real greater values of critical velocities and real smaller amplitudes are safer for structures.

References

Błazik-Borowa, E. and Flaga, A. (1996), "Modelling of aerodynamic loads on a downstream cylinder caused by bistable flow between two circular cylinders", *J. Wind Eng. Ind. Aerodyn.*, **65**, 361-370.

Błazik-Borowa, E. and Flaga, A. (1998), "Numerical analysis of interference galloping of two identical circular cylinders", *Wind and Struct., An Int. J.*, **1**(3), 243-253.

Błazik-Borowa, E. and Szulej, J. (2004), "The estimation of errors for simulation of wind velocity fields", *Proceeding of IV Symposium Environmental Effects on Buildings and People,* Lublin University of Technology, 51-54.

Borri, C., Crocchini, F., Facchini, L. and Spinelli, P. (1995), "Numerical simulation of stationary and

nonstationary stochastic processes: a comparative analysis for turbulent wind fields", *Proceedings of 9th ICWE, "Retrospect and Prospect"*, **1**, New Delhi, 47-55.
Bourdeix, M.T., Hémon, P. and Santi F. (1998), "Wind induced vibrations of chimneys using an improved quasi-steady theory for galloping", *J. Wind Eng. Ind. Aerodyn.*, **74-76**, 785-794.
Brika, D. and Laneville, A. (1995), "Wake interference between two circular cylinders", *Proccedings of 9ICWE*, New Delhi, 153-164.
Brun, C., Tenchine, D. and Hopfinger, E.J. (2004), "Role of the shear layer instability in the near wake behaviour of two side-by-side circular cylinders", *Experiments in Fluids*, **36**, 334-343.
ESDU 84015 (1984), Cylinders groups: mean forces on pairs of long circular cylinders", *Eng. Sci. Data*, August 1984.
Flaga, A. (1994), "Quasisteady models of wind load on slender structures. Part 1. Case of a motionless structure", *Archives of Civil Engineering*, XL, 1, str. 3-28.
Gowda, B.H.L., Sreedharan, V. and Narayanan, S. (1993), "Vortex induced oscillatory response of a circular cylinder due to interference effects", *J. Wind Eng. Ind. Aerodyn.*, **49**, 157-166.
Ikegami, Y., Fujita, K. and Ohashi, M. (1993), "Nozzle jet flow-induced vibration of single circular cylinders and twin circular cylinders", *J. Wind Eng. Industrial Aerodyn.*, **49**, 207-216.
Jester, W. and Kallinderis, Y. (2003), "Numerical study of incompressible flow about fixed cylinder pairs", *J. Fluids Struct.*, **17**, 561-577.
Kazakiewicz, J. (1987), *Aerodinamika Mostow*, Moscow "Transport".
Matsumoto, M., Shiraishi, N. and Shirato, H. (1990), "Aerodynamic instabilities of twin circular cylinders", *J. Wind Eng. Ind. Aerodyn.*, **33**, 91-100.
Ng, C.W., Cheng, V.S.Y. and Ko, N.W.M. (1997), "Numerical study of vortex interactions behind two circular cylinders in bistable flow regime", *Fluid Dynamics Res.*, **19**, 379-409.
Park, C.W. and Lee, S.J. (2003), "Flow structure around two finite circular cylinders located in an atmospheric boundary layer: side-by-side arrangement", *J. Fluids Struct.*, **17**, 1043-1058.
Ruscheweyh, H. and Dielen, B. (1992), "Interference galloping- investigations concerning the phase lag of the flow switching", *J. Wind Eng. Ind. Aerodyn.*, **41-44**, 2047-2056.
Shinozuka, M. and Jan, C. M. (1972), "Digital simulation of random processes and its application", *J. Sound Vib.*, **25**(1), 111-128.
Studnicková, M. (1994), "Induced vibrations of leeward ropes - a practical examples", *Proceedings of East European Conference on Wind Eng.*, Part 1, **3**, Warsaw, 157-167.
Zdravkovich, M.M. and Pridden, D.L. (1977), "Interference between two identical circular cylinders; Series of unexpected discontinuities", *J. Ind. Aerodyn.*, **2**, 255-270.
Zdravkovich, M.M. (1987), "Review of interference - induced oscillations in flow past two parallel circular cylinders in various arrangements", *Proceedings of Seventh International Conference on Wind Eng.*, **2**, Aachen, 51-66.
Zdravkovich, M.M. and Medeiros, E. (1991), "Effect of damping on interference-induced oscillations of two identical circular cylinders", *J. Wind Eng. Ind. Aerodyn.*, 197-211.
Zhang, H. and Melbourne, W.H. (1995), "Effects of free stream turbulence on flow interference between two circular cylinders in side-by-side arrangement", *Proceedings of Ninth International Conference on Wind Eng.*, New Delhi, 141-152.

GS